SEISMIC PERFORMANCE OF RC SHEAR WALLS WITH MULTI-OPENINGS

Masato SAKURAI[1], Hiroshi KURAMOTO[2], Tomoya MATSUI[3] and Tomofusa AKITA[4]

[1] *Graduate School of Engineering, Toyohashi University of Technology, Toyohashi, Japan*
[2] *Prof., Dept. of Architectural Engineering. Osaka University, Suita, Japan*
[3] *Assistant Prof., Dept. of Architecture and Civil Eng., Toyohashi University of Technology, Toyohashi, Japan*
[4] *Assistant Prof., Dept. of Architecture, Chiba University, Chiba, Japan*

Email: m053620@edu.imc.tut.ac.jp, matsui@tutrp.tut.ac.jp, kuramoto@arch.eng.osaka-u.ac.jp, akita@faculty.chiba-u.jp

ABSTRACT:

This paper outlines a static loading test of RC shear walls with openings carried out to investigate the influence of different number and layout of the openings. All specimens have the same equivalent perimeter ratio of openings, that is 0.4. The test results showed that the shear strength, failure mode and deformability of RC shear walls with openings were significantly affected by the difference of the number and layout of openings. It was also observed that the overturning moment at the bottom of the shear walls with openings were smaller than those of without opening because the rotation at the bottom of the shear walls with openings became smaller due to the existence of the openings. FEM analysis was also conducted to simulate the hysteresis loops and failure progress of the shear walls with openings, and good agreement between experimental and analytical results was obtained.

KEYWORDS: RC shear walls with openings, Static test, Seismic performance, Shear strength, FEM analysis

1. INTRODUCTION

In general, the shear strength of RC shear walls with openings are evaluated by using an equivalent perimeter ratio of openings in the AIJ design standard for RC structures in Japan. Although the opening layouts are different, the shear strength of shear walls with the same value of the equivalent perimeter ratio is calculated by using the above method. As for the existing experimental results and the earthquake damage to RC buildings in the past, the failure mechanisms of RC shear walls with openings are complicated. Especially, in case of those with multi-openings, the quantitative evaluation of the seismic performance is very difficult even in the present.

The main objective of this study is to grasp the seismic performance of the walls, such as failure mode, hysteresis characteristic and deformability in order to improve the evaluation method of the shear strength for RC shear walls with multi-openings. In this paper, results of a static loading test carried out on RC shear walls with openings, to compare the difference in number and layout of the openings were discussed. In addition, the numerical simulation was performed by FEM analysis in order to compare the test results.

2. EXPERIMENTAL PROGRAM

2.1 specimens

The specimens are designed to simulate the lower two story of multi-story shear wall in medium-rise RC building and scaled to one-third of the prototype walls. Details of the section and configuration of specimens are shown in Table 1 and Figure 1. Basic specifications were similar to the specimen of shear wall without opening tested in previous study (Akita T. et al., 2006) [1]. Variables investigated were the number and layout of the openings. Specimen WO1 has one opening, while Specimen WO2 and WO3 have two openings. The two openings in Specimen WO2 are positioned close to one another, while those in Specimen WO3 are at a distance, as shown in Fig.1. The equivalent perimeters ratios of openings were almost same for all specimens, i.e 0.4. The mechanical properties of materials used are listed in Table 2.

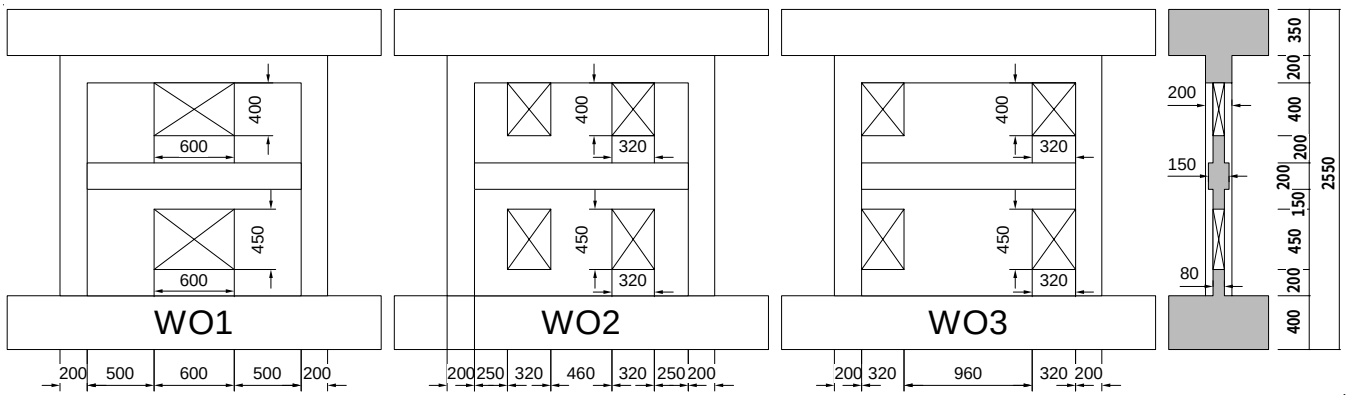

Figure 1 Test Specimens

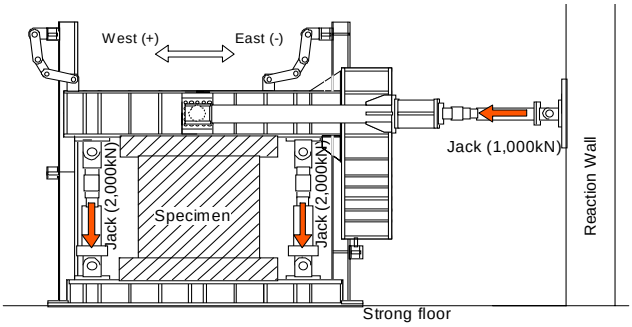

Figure 2 Loading apparatus

2.2 Loading method

The loading apparatus used is shown in Fig.2. The wall specimens were loaded horizontal shear reversals by a manual jack of 1,000kN capacity with applying constant axial force of 442kN by two vertical manual jacks of 2,000kN capacity for each. During the testing, the additional moment was also applied to the top of specimens using vertical jacks to keep the prescribed shear-span ratio of 1.38.

The loading was conducted by controlling the relative wall drift angle, R, given by the ratio of the height of corresponding to the measuring point of horizontal displacement at the top of the specimen, *h* (2,000mm), to the horizontal deformation, δ, i.e. R=δ/ *h*.

2.3 Measurement

Displacement transducers were used to measure horizontal displacement of upper stub, longitudinal deformation of column and deformation of wall panel. The strain of longitudinal and transverse reinforcement of columns and walls are measured by using strain gauges. In addition, the crack widths are measured by using crack scale at peak in each loading and unloading cycles.

Table 1 Specification of section

		First story	Second story
Column	B×D	200×200	
	Longitudinal bar	12-D13 (pg=3.8%)	
	Tie	2-D6@60 (pw=0.53%)	2-D6@50 (pw=0.64%)
	Sub-tie	2-D6@120 (pw=0.27%)	-
Beam	B×D	150×200	200×500*1
	Longitudinal bar	4-D10 (pt=0.54%)	
	Stirrup	2-D6@100 (pw=0.42%)	
Wall	Thickness	80	
	Longitudinal bar	D6@100zigzag (ps=0.4%)	
	Transverse bar	D6@100zigzag (ps=0.4%)	
	Bar around opening	D10 (longitudinal, horizontal, diagonal)	

Unit: mm, F_c=27MPa
*1 Upper 300mm of beam depth 500mm has combined with an upper stub
longitudinal bar of column (SD390), other (SD295A)

Table 2 Properties of material used

Steel bar		Yield strength (N/mm^2)	Young's modulus (kN/mm^2)	Ultimate strength (N/mm^2)
D6 (SD295A)	Wall reinforcement, tie, stirrup	336	211	565
D10 (SD295A)	Beam reinforcement, Opening reinforcement	327	163	439
D13 (SD390)	Column reinforcement	422	173	562
concrete		WO1	WO2	WO3
σ_B (N/mm^2)	First story	32.9	34.7	34.9
	Second story	29.7	29.5	28.6

3. TEST RESULTS

3.1 Damage process and hysteresis loop

Cracking patterns of each specimen after the loading cycle of 1/133 rad. are shown in Fig.3. The loading toward the west direction (Fig. 2) is defined as the positive loading while the loading toward the east direction is the negative loading. The shear force versus drift angle relationships of the three specimens are shown in Fig.4

For each specimen, the initial crack occurred at the wing wall and column in the first story in the loading cycle of 1/1600 rad. The flexural cracks increased at the column in the first story in the loading cycle of 1/800 rad., and new cracks occurred to wing wall in the second story. The cracks propagated throughout the wall and the column in the loading cycle of 1/400 and 1/200 rad..

In Specimen WO1 with one opening, the maximum shear force reached 542kN at R of 1/133 rad., and –543kN at R of -1/133 rad., and the shear crack widths from the first story to the second story over the beam increased particularly. The falling of concrete in the wing wall of second story occurred significantly in the loading cycle of 1/100 rad., and the wing wall of the second story failed in compression. Then, significant capacity degradation was observed. Finally, Specimen WO1 failed in the loading cycle of 1/33 rad. due to shear failure of column in the second story.

For Specimen WO2 with two openings, the maximum shear force reached -469kN at R of -1/200 rad., and 474kN at R of 1/133rad. The Shear cracks of the central panels in the first and second story propagated particularly, and the spalling of cover concrete in this panel occurred in the loading cycle of 1/133 rad.. The central panels in the first and second story failed in shear with capacity deterioration in the loading cycle of 1/100 rad., and the wing wall in the first story failed in compression in the loading cycle of 1/67 rad.. After the loading cycle of 1/50 rad., Specimen WO2 maintained the capacity of about 250kN until the last loading cycle of 1/20 rad. might be due to resisting flexural strength of the column from damage process.

In Specimen WO3, a capacity deterioration was observed after reaching the maximum shear force of 555kN, at R of 1/133 rad., and –552kN at R of -1/133 rad.. The central panel in the second story failed in shear with significant falling of concrete in the loading cycle of 1/100 rad., and the columns in second story failed in shear in the loading cycle of 1/67 rad..

As described above, although the three specimens fail in shear eventually, the failure progress of the shear walls with openings was different.

3.2 Calculated ultimate strength

The calculated flexural strength and shear strength of the specimens are shown in Fig. 4 and Table 3. The calculated flexural strength Q_{mu} is given by Eq. (3.1) [2]. The calculated shear strength, Q_{su1} (Eq. (3.2)), is given by multiplying shear strength of non-opening shear walls by reduction factor γ using equivalent perimeter ratio in AIJ design standard for RC structure [3]. The calculated shear strength, Q_{su2} (Eq. (3.4)), is an estimation

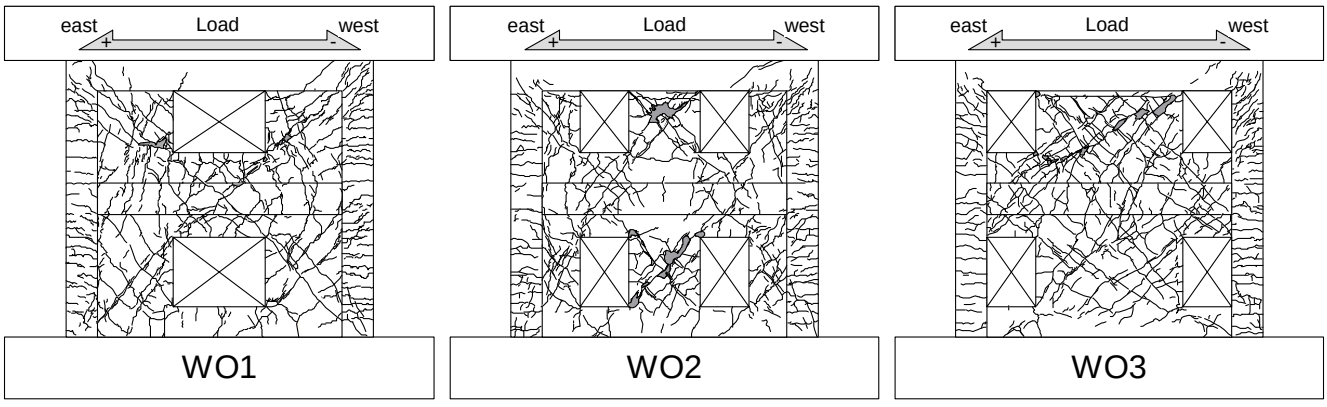

Figure 3 Cracking situation after loading cycle of R=1/133 rad. (Test)

proposed by Ono and Tokuhiro [4]. Used signatures in Eq. (3.3) and (3.5) are shown in Fig.5, where A_e is diagonal compression field in the shear wall with openings.

$$Q_{mu} = \left(a_t \cdot \sigma_y \cdot l_w + 0.5\, a_w \cdot \sigma_{wy} \cdot l_w + 0.5\, N \cdot l_w\right) / h \tag{3.1}$$

$$Q_{su1} = \gamma \left\{ \left[\frac{0.053\, p_{te}^{0.23} \cdot (F_c + 18)}{M/(Q \cdot l) + 0.12} + 0.85\sqrt{\sigma_{wh} \cdot p_{se}} + 0.1\sigma_{0e} \right] \cdot b_e \cdot j_e \right\} \tag{3.2}$$

$$\gamma = \left\{ 1 - \sqrt{\frac{\sum h_i \cdot l_i}{hl}} \right\} \tag{3.3}$$

$$Q_{su2} = \gamma_u \left\{ \left(2.4\sqrt{F_c} + 3400 P_s\right) \cdot t \cdot l \right\} \tag{3.4}$$

$$\gamma_u = \sqrt{\frac{\sum A_e}{hl}} \tag{3.5}$$

Every specimen didn't reach the calculated flexural strength, which means that the capacity of the specimens is given by their shear strength. The ratio of the measured maximum shear force to calculated strength, Exp./Q_{su1}, were 2.32 for Specimen WO1, 1.97 for Specimen WO2 and 2.30 for Specimen WO3, and the shear strength of three specimens was lager than calculated shear strength, respectively. On the other hand, Exp./Q_{su2} were 1.04 for Specimen WO1, 1.27 for Specimen WO2 and 1.18 for Specimen WO3, while the calculated shear strength, Q_{su2} was good agreement with the maximum shear force for all three specimens, respectively.

3.3 Behavior of the bottom of wall

The deformation distributions at the bottom of wall at the R of +1/400 rad., +1/200 rad. and +1/133 rad. for each specimen are shown in Fig.6 (plus = tension, minus = compression). As a reference, the result of Specimen AS (shear wall without opening) in previous study is shown in Fig.6. The locations of

Table 3 calculated strength

	Peak load(Exp.) (kN)		Q_{mu} (kN)	Exp./ Q_{mu}	Q_{su1} (kN)	Exp./ Q_{su1}	Q_{su2} (kN)	Exp./ (Q_{su2})
	(+)	(−)						
WO1	542	-543	618	0.88	233	2.32	522	1.04
WO2	473	-469	618	0.77	240	1.97	372	1.27
WO3	555	-552	618	0.90	240	2.30	471	1.18

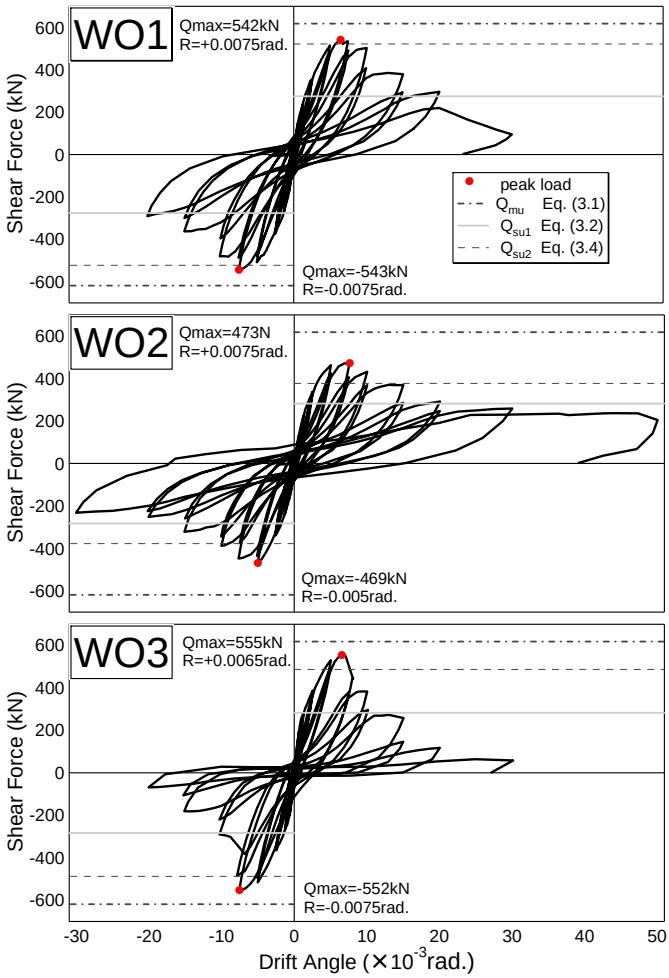

Figure 4 Hysteresis loops (Test)

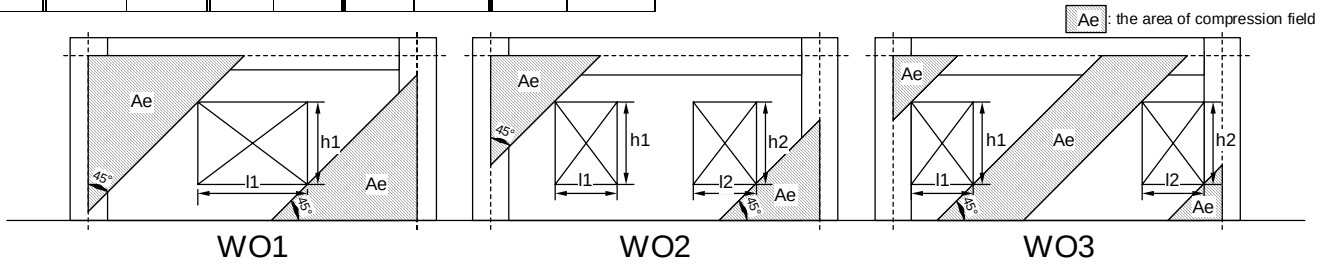

Figure 5 Used signatures in Eq. (3.3) and (3.5)

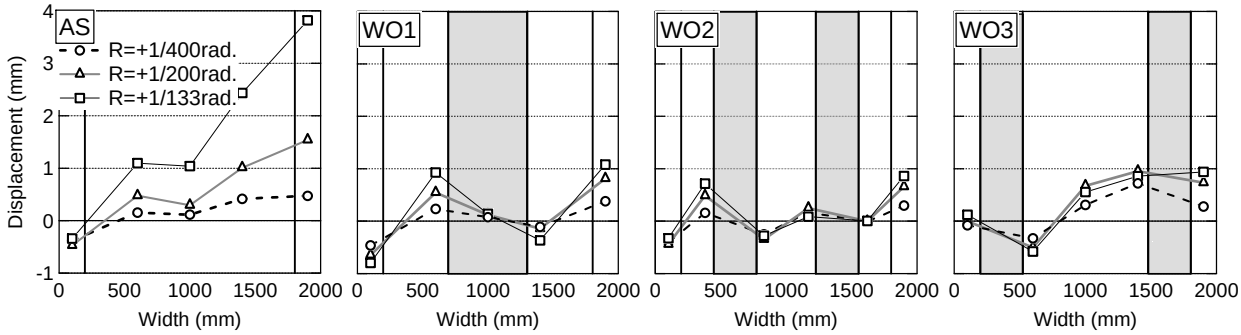

Figure 6 Deformation distributions (bottom of walls)

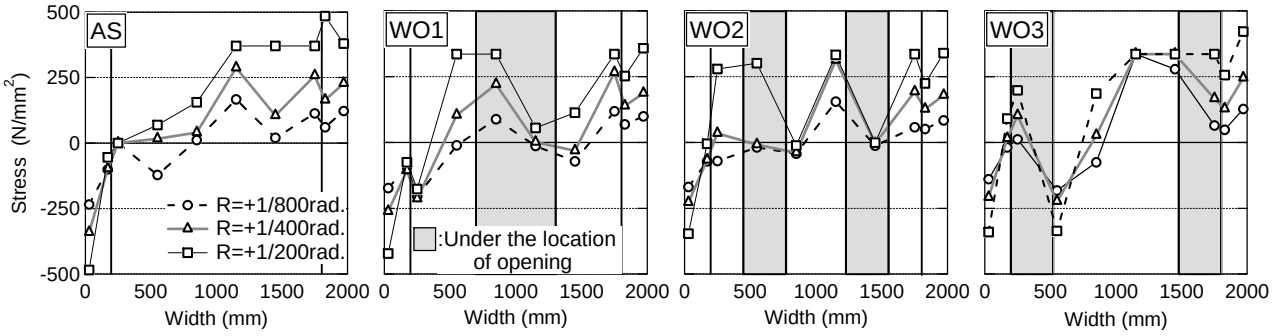

Figure 7 Stress distributions (bottom of walls)

measured displacement on the specimens are shown in Fig.8.

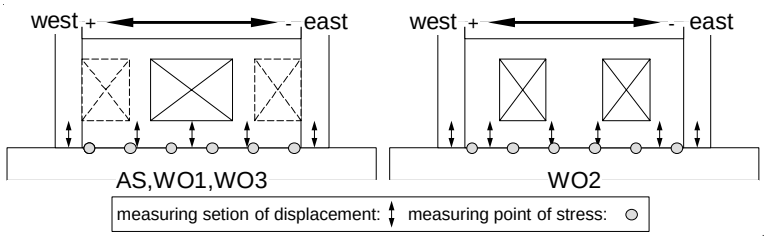

Figure 8 Location of measuring

For all specimens, the deformations of west columns were in compressive, while in the east columns were in tensile. Deformation of the east column for Specimen AS was about 4mm at R of 1/133rad., while those for Specimens WO1, WO2 and WO3 were less than 1mm. The openings made a remarkable difference to the deformation level. On the other hand, it is found that the wing walls of Specimen WO1 rotated individually. Similar to Specimens WO1, the wing walls and central walls of Specimen WO2 and WO3 also rotated individually. This indicated that shear walls without opening and shear walls with openings were clearly difference in deformation at the bottom of the wall.

The stress distributions of longitudinal bar at the bottom section of walls and columns at the R of +1/800 rad., +1/400 rad. and +1/200 rad. are shown in Fig.7 (plus = tension, minus = compression). The locations of measured stress on the specimens are also shown in Fig.8. On the assumption that the history loop of a steel bar is bilinear, the stress was calculated using strain measured by the strain gauge.

The stress of west column was in compressive, and that of east column was in tensile for each specimen. These results have a similar tendency for the deformation distribution. The stress distribution of each member; the columns, columns with wing wall and central wall panels sloped down to the left caused by localized rotations. Therefore, each member contributed to the overturning moment individually. On the other hand, the stress distribution of shear wall without opening (Specimen AS) in tensile increased gradually from the west side to the east side, where the overturning moment at the bottom of the shear walls was borne by the whole bottom of wall.

Consequently, the stress and deformation distributions at the bottom of shear walls with openings (Specimen WO1, WO2 and WO3) were different from that shear walls without opening. This indicated that the base moment of shear walls with openings was smaller than that of non-opening shear wall. In addition, it was

confirmed that the difference of layout and number of openings made a difference to stress state at the bottom of shear walls.

4. NON-LINEAR FEM ANALYSIS

4.1 Analytical Model

A two-dimensional non-linear FEM analysis was also conducted for all specimens. The validity of analytical model is examined to investigate the stress transfer mechanism of RC Shear wall with multi-openings. The finite element model was calibrated against experimental results. The finite element mesh for Specimen WO1 is shown in Fig.7. Each node at the bottom end of the under stub had pin support to restrain vertical and lateral displacement. The elements between the loading point prescribed shear-span ratio of 1.38 and the top end of upper stub were defined as an elastic body, which is a virtual stub. A node at the top of the virtual stub was subjected to lateral displacement reversals with applying a constant initial axial force of 442kN. The FEM non-linear analysis software "FINAL" [5] was used in this analysis.

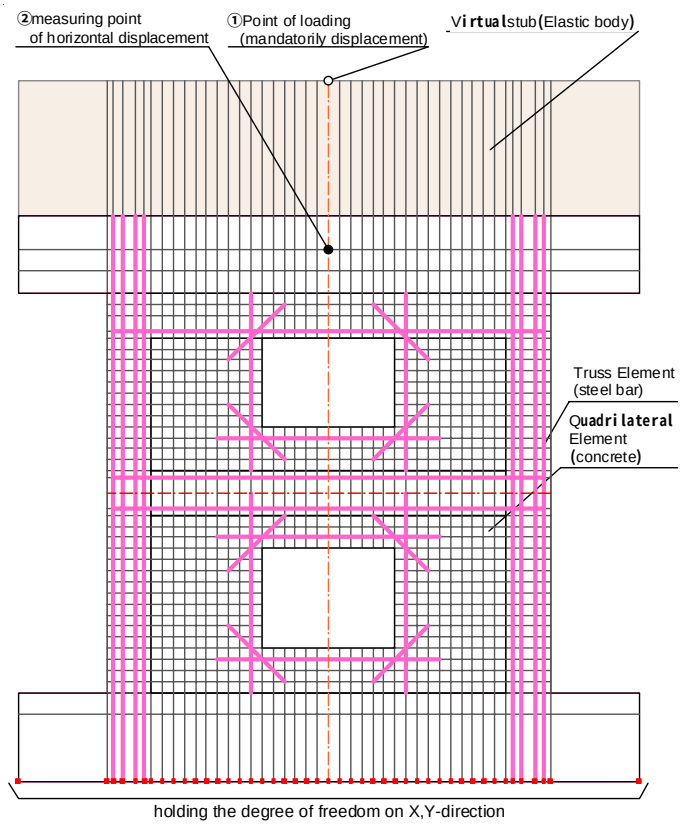

Figure 8 Finite element mesh (specimen WO1)

4.2 Element Model

Mechanical properties of material model used in the analysis are listed in Table 2 and table 4. The quadrilateral plane stress element was used for concrete. Reinforcing bars in the wall panel and stirrup of the column and beam are substituted equivalent layers with stiffness in the bar direction and superposed on the quadrilateral elements. Longitudinal bar in the column and beam were modelled by the truss elements. Line element was used between the truss elements and the quadrilateral elements to consider the bond slip.

The material model of steel was a plasticity model, which was the Von Mises model failure surface with associated plastic rule. The stress-strain curve of the steel was idealized by the Modified Menegotto-Pinto model by Ciampi, and the isotropic hardening rule was adopted as the hysterical model.

As for the stress-strain relationship of concrete, a modified Ahmad model was adopted for the compressive stress-strain curve. The model by Kupher and Gerstle was adopted as the fracture

Table 4 Mechanical properties used in the analysis

		σ_c (N/mm^2)	F_t (N/mm^2)	
			calculated	modified
WO1	First story	32.9	1.89	0.95 (column, beam)
	Second story	29.7		0.47 (wall panel)
WO2	First story	34.7	1.94	0.97 (column, beam)
	Second story	29.5		0.49 (wall panel)
WO3	First story	34.9	1.95	0.97 (column, beam)
	Second story	28.6		0.49 (wall panel)

		E_c (N/mm^2)		ε_{c0} (μ)	
		calculated	modified	calculated	modified
WO1	First story	26500	13200	2140	4000
	Second story	25400	12700	2096	
WO2	First story	27000	13500	2165	
	Second story	25300	12700	2094	
WO3	First story	27100	13600	2168	
	Second story	25100	12600	2081	

σ_c：Compressive strength、F_t：stress at crack，$F_t=0.33\sqrt{(\sigma_c)}$,

E_c：elastic modulus，$E_c=(0.36\sqrt{(\sigma_c)}+0.582)*10^4$ (AIJ standard),

ε_{c0}：strain at compressive strength，$\varepsilon_{c0}=13.7\sigma_c+1690$

criterion of concrete under biaxial stress state [6], and the compressive strength reduction factor was adopted from Naganuma [7]. The concrete tension stiffing model determined as a function of the compressive stress and reinforcement ratio proposed by Naganuma was adopted in the tensile zone [7]. The tensile strength of concrete was reduced to consider influence of desiccation shrinkage. The Naganuma model was adapted as the shear transfer model after cracks occurred in the concrete element [7].

As a result of conducting an analysis using the above constitutive laws, strength in the analysis deteriorated earlier than that of in the experimental result. Therefore, calculated elastic modulus E_c and strain at compressive strength of concrete were reduced, as listed in Table.4

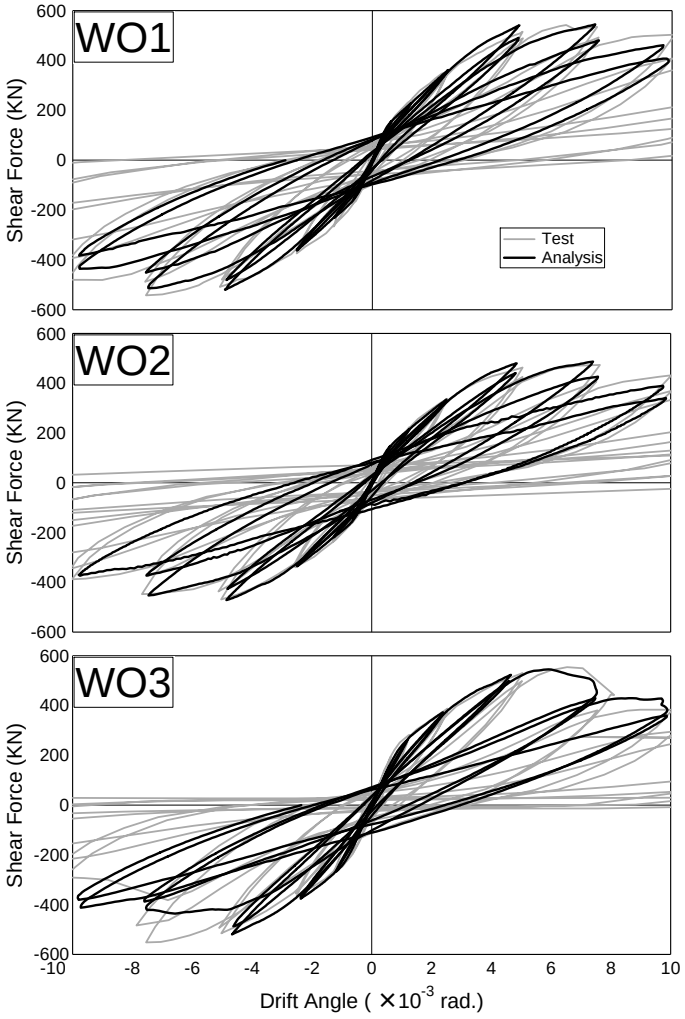

Figure 9 Hysteresis loop
(Comparison Analysis and Test)

4.3 Comparison Analysis with Test

The shear force versus drift angle relationship in the experiment and analysis for the specimens until R of 1/100 rad. are shown in Fig.9. Although the initial stiffness in the analysis was evaluated to be slightly larger than the experimental, the analytical backbone curve agreed well with the experimental results until R of 1/133 rad. The maximum shear forces in the analysis were almost the same as in the experimental value in each specimen. However, the correspondence between the analytical backbone curve and experimental ones decreased after the peak load. This is one of the reasons for the difficulty to simulate the strength deterioration caused by failure of concrete after the maximum strength in the analysis. However, it is confirmed that this analysis reproduced the backbone curve in the experiment with sufficient accuracy until the peak load.

Cracking situations of each specimen on the analysis after the loading cycle of 1/133 rad. are shown in Fig.10. Because tensile strength of concrete was reduced to consider the influence of desiccation shrinkage in the analysis, the analytical initial crack occurred earlier than that of in the experiment. On the other hand, comparing cracking situation in Fig.3, the analytical damage situations of concrete at the peak load agreed well

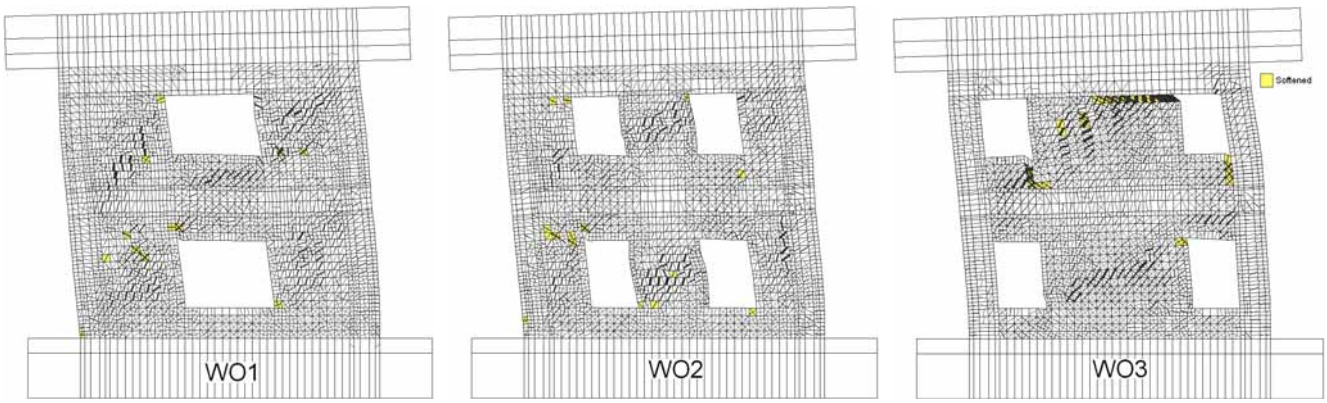

Figure 10 Cracking situation after the loading cycle of R=1/133 rad. (Analysis)

with the experimental one. In addition, the large damage of concrete at the corner of wing walls for Specimens WO1 and at the corner of central panel for Specimens WO2 can be seen in the analysis agreed with in the experimental. The analysis can simulate the damage situation properly. Therefore, the backbone curve and failure progress of the shear wall with openings agreed well with experimental results. It is confirmed that FEM analysis using these analytical model and constitutive low can simulate the behavior of the shear wall with openings with sufficient accuracy until the peak load. Moreover, the inner stress state of the shear wall with opening will be examined using these analytical results in next phase of the research.

5. CONCLUSIONS

In this paper, a static loading test of RC shear walls with openings was carried out to compare the difference in number and layout of the openings. In addition, the numerical study was performed by FEM analysis to compare the test results. The following conclusions can be drawn.

1) The shear strength, failure mode and deformability of RC shear walls with openings were significantly affected by the difference of the number and layout of openings.

2) The calculated shear strength of RC shear walls with opening by equivalent perimeter ratio is in the safety limit, but its predictive accuracy is not so adequate. On the other hand, proposed estimation by Ono and Tokuhiro is good agreement with the shear strength in the experiment.

3) The axial deformation and stress distribution at the bottom of shear walls with opening were different from those without opening, where columns, wing walls, central panels of the wall contribute to its base moment.

4) The RC shear wall with openings was simulated by FEM analysis to produce the backbone curve and failure progress, and good agreement between experimental and analytical results was identified.

REFFERENCES

[1] Akita, T., Kuramoto, H., Matsui T., and Kabeyasawa. T. (2006). Hysteresis Modeling of RC Shear Walls Based on Static Loading Test. *Proceedings of the 8th U.S. National Conference on Earthquake Engineering (8NCEE)* Paper No. 1291.

[2] Japan Building Disaster Prevention Association (2001). Evaluation Standard of Seismic Capacity on Existing RC Buildings, Japan.

[3] Architectural Institute of Japan. (2000). AIJ Standards for Structural Calculation of steel Reinforced Concrete Structures, Japan.

[4] Ono, M. and Tokuhiro, I. (1992). A Proposal of Reducing Rate for Strength due to Opening Effect of Reinforced Concrete Framed Shear Walls. *Journal of structural and construction engineering.* No.435. 119-129.

[5] “FINAL/99”. ITOCHU Techno-Solutions Corporation

[6] Kupfer, B., and Gerstle, H. et al. (1973) Behavior of Concrete Under Biaxial Stress. *Journal of the engineering mechanics division.* 853-866

[7] Naganuma, K. (1991). Nonlinear Analytical Model for Reinforced Concrete Panels Under In-Plane Streses *Journal of structural and construction engineering.* No.421. 39-48.